

Article

## Solid-State Synthesis and Photocatalytic Activity of Polyterthiophene Derivatives/TiO<sub>2</sub> Nanocomposites

Ruxangul Jamal <sup>1,2</sup>, Yakupjan Osman <sup>1,2</sup>, Adalet Rahman <sup>1,2</sup>, Ahmat Ali <sup>1,2</sup>, Yu Zhang <sup>1,2</sup> and Tursun Abdiryim <sup>1,2,\*</sup>

<sup>1</sup> Key Laboratory of Petroleum and Gas Fine Chemicals, Educational Ministry of China, College of Chemistry and Chemical Engineering, Xinjiang University, Urumqi 830046, Xinjiang, China; E-Mails: jruxangul@sina.com (R.J.); jakobosm@gmail.com (Y.O.); Adaletr@sohu.com (A.R.); ahmatjanchem@126.com (A.A.); zhyurainy@163.com (Y.Z.)

<sup>2</sup> Key Laboratory of Functional Polymers, Xinjiang University, Urumqi 830046, Xinjiang, China

\* Author to whom correspondence should be addressed; E-Mail: tursunabdir@sina.com.cn; Tel./Fax: +86-991-8583-575.

Received: 6 November 2013; in revised form: 14 April 2014 / Accepted: 7 May 2014 /

Published: 14 May 2014

---

**Abstract:** Poly(3,4-propylenedioxy-2,2':5',2''-terthiophene)/TiO<sub>2</sub> and poly(3,4-(2,2-dimethylenepropylenedioxy)-2,2':5',2''-terthiophene)/TiO<sub>2</sub> nanocomposites were synthesized by a simple solid-state method. Additionally, the poly(3,4-propylenedioxy thiophene)/TiO<sub>2</sub> and poly(3,4-2,2-dimethylenepropylenedioxythiophene)/TiO<sub>2</sub> nanocomposites were synthesized in a similar manner for comparison. The structure and morphology were characterized by Fourier transform infrared (FTIR), ultraviolet-visible (UV-Vis) absorption spectroscopy, X-ray diffraction (XRD) and transmission electron microscopy (TEM). The photocatalytic activities of the nanocomposites were examined through the degradation processes of a methylene blue (MB) solution under UV light and sunlight irradiation. The results of FTIR and UV-Vis spectra showed that the composites were successfully synthesized by solid-state method and the poly(3,4-propylenedioxy-2,2':5',2''-terthiophene)/TiO<sub>2</sub> and poly(3,4-(2,2-dimethylenepropylenedioxy)-2,2':5',2''-terthiophene)/TiO<sub>2</sub> nanocomposite had a higher oxidation degree and conjugation length than others. The results also indicated that the TiO<sub>2</sub> had no effect on the crystallinity of composites, but was well embedded in the polymer matrix. Additionally, the highest degradation efficiency of 90.5% occurred in the case of the poly(3,4-propylenedioxy-2,2':5',2''-terthiophene)/TiO<sub>2</sub> nanocomposite.

**Keywords:** polyterthiophene derivative; nano-TiO<sub>2</sub>; solid-state method; photocatalyst

---

## 1. Introduction

The use of semiconducting materials in environmental decontamination as photocatalysts has attracted a great deal of attention in recent years [1]. When semiconducting materials are exposed to light with energy larger than their band gaps, electron-hole pairs can be created, which can initiate photocatalytic reactions [2]. Most photocatalytic systems are based on TiO<sub>2</sub>, which is chemically stable and has a long life-time of electron-hole pairs generated by optical excitation. However, the band gap of TiO<sub>2</sub> is ~3.2 eV, which is in the ultraviolet regime, and therefore, visible light, which comprises most of the solar light, cannot be absorbed by TiO<sub>2</sub> [3]. To overcome this problem, some strategies have been investigated, including noble metal deposition, the doping of metal or nonmetal ions, mixing with another metal oxide, surface photosensitization with dye and preparing composites with a conducting polymer [4–6]. Conducting polymers have attracted considerable attention, because of their interesting semiconducting, electronic and optical properties [7]. Among conducting polymers, polyaniline and polythiophene are widely used for the fabricating of conducting polymer/TiO<sub>2</sub> hybrid materials [8,9]. Polythiophene and its derivatives show many advantages in combining with TiO<sub>2</sub>, and the large internal interface area in the polythiophene/TiO<sub>2</sub> composite enables an efficient separation of charge, which is very important for photovoltaic application [10,11]. At the present time, numbers of reports have been published on the preparation of polythiophene and its derivatives/TiO<sub>2</sub> composites, including original *in situ* photopolymerization [12], electrochemical polymerization [13] and the chemical solution method [14]. Although polythiophene has become the focus of considerable interest, polythiophene suffers from the occurrence of undesired  $\alpha,\beta$ - and  $\beta,\beta'$ -couplings during polymerization, which deteriorate their electronic and optical properties [15,16]. As derivatives of polythiophene, polyterthiophene-type conjugated polymers have rapidly gained considerable attention, due to the preexistence of  $\alpha,\alpha'$ -linkages in their monomers, which makes the whole polyterthiophene-type chain grow regularly and leads to very interesting electronic, electrochromic and optical properties [17–19]. Additionally, they can be prepared by electrochemical and chemical methods. Recently, we have demonstrated a novel room-temperature solid-state oxidative method for the polymerization of ethylenedioxy-substituted terthiophene, and we have found that solid-state polymerization was an effective method for the polymerization of the terthiophene-type monomer [20].

In this paper, we selected 3,4-propylenedioxy-2,2':5',2''-terthiophene and 3,4-(2,2-dimethylenepropylenedioxy)-2,2':5',2''-terthiophene as monomers for the preparation of the polyterthiophene derivatives/TiO<sub>2</sub> nanocomposites. As these monomers have  $\alpha,\alpha'$ -linkages, it can be deduced that the resulting polymers may grow regularly and will have a high absorption coefficient and a wide absorption wavelength in the visible part of the spectrum, which will allow the TiO<sub>2</sub> photocatalyst to harvest incident light efficiently in composite photocatalyst. Furthermore, these monomers are in a solid state, and they can be polymerized by the solid-state method. In the present work, with the aim of the above consideration, the room-temperature solid-state polymerization method was applied for the oxidative polymerization of the above terthiophene monomers,

3,4-propylenedioxy-2,2':5',2''-terthiophene (TPT) and 3,4-(2,2-dimethylenepropylenedioxy)-2,2':5',2''-terthiophene (TMPT), for the preparation of the poly(3,4-propylenedioxy-2,2':5',2''-terthiophene)/TiO<sub>2</sub> (poly(TPT)/TiO<sub>2</sub>) and poly(3,4-(2,2-dimethylenepropylene-dioxy)-2,2':5',2''-terthiophene)/TiO<sub>2</sub> (poly(TMPT)/TiO<sub>2</sub>) nanocomposites. Additionally, the poly(3,4-propylenedioxythiophene)/TiO<sub>2</sub> (PProDOT/TiO<sub>2</sub>) and poly(3,4-2,2-dimethylene-propylenedioxythiophene)/TiO<sub>2</sub> (PProDOT-Me<sub>2</sub>/TiO<sub>2</sub>) nanocomposites were synthesized in a similar manner for comparison. The structure and properties of the nanocomposites were investigated by FTIR, UV-Vis and X-ray diffraction. In addition, the photocatalytic activities of the nanocomposite were evaluated by the degradation processes of a methylene blue (MB) solution under UV light and sunlight irradiation.

## 2. Results and Discussion

### 2.1. Fourier Transform Infrared (FTIR) Spectra

Figure 1 gives the FTIR spectra of solid-state synthesized PProDOT/TiO<sub>2</sub>, PProDOT-Me<sub>2</sub>/TiO<sub>2</sub>, poly(TPT)/TiO<sub>2</sub>, poly(TMPT)/TiO<sub>2</sub> and nano-TiO<sub>2</sub>. As can be seen in Figure 1, the bands for PProDOT/TiO<sub>2</sub> and PProDOT-Me<sub>2</sub>/TiO<sub>2</sub> are as follows: ~1650, ~1490, ~1320, ~1167, ~1125, ~1045, ~920, ~838 and ~706 cm<sup>-1</sup>. The bands at ~1650, ~1490 and ~1320 cm<sup>-1</sup> are assigned to the characteristic bands of the thiophene ring [20]. The bands appearing at ~1167, ~1125 and ~1045 cm<sup>-1</sup> are associated with the C–O–C bending vibration in the propylene oxide group [21,22], while the bands at ~916, ~838 and ~706 cm<sup>-1</sup> are the characteristic bands of the stretching vibrations of the C–S–C bond in the thiophene ring [23–25], which are similar to the previously reported IR spectrum of PProDOT [26,27]. Furthermore, comparing the FTIR spectra of poly(TPT)/TiO<sub>2</sub> and poly(TMPT)/TiO<sub>2</sub> with that of PProDOT/TiO<sub>2</sub> and PProDOT-Me<sub>2</sub>/TiO<sub>2</sub>, one can see that the positions of the main IR bands of poly(TPT)/TiO<sub>2</sub> and poly(TMPT)/TiO<sub>2</sub> nanocomposites are nearly identical with that of PProDOT/TiO<sub>2</sub> and PProDOT-Me<sub>2</sub>/TiO<sub>2</sub>. However, the bands of the poly(TPT)/TiO<sub>2</sub> and poly(TMPT)/TiO<sub>2</sub> nanocomposites at ~1496, ~1170 and ~832 cm<sup>-1</sup> are shifted slightly from their corresponding position to the lower wavenumber compared with that of the PProDOT/TiO<sub>2</sub> and PProDOT-Me<sub>2</sub>/TiO<sub>2</sub> nanocomposites, which indicates that the higher oxidation degree and stronger interaction between the TiO<sub>2</sub> with polymer occur in the case of the poly(TPT)/TiO<sub>2</sub> and poly(TMPT)/TiO<sub>2</sub> nanocomposites, as compared to the PProDOT/TiO<sub>2</sub> and PProDOT-Me<sub>2</sub>/TiO<sub>2</sub> nanocomposites [28]. In addition, a close look will reveal that the characteristic peak of TiO<sub>2</sub> at ~3410 cm<sup>-1</sup> is appearing in the case of PProDOT/TiO<sub>2</sub> and PProDOT-Me<sub>2</sub>/TiO<sub>2</sub> nanocomposites. However, there is no characteristic peak corresponding to the TiO<sub>2</sub> in the poly(TPT)/TiO<sub>2</sub> and poly(TMPT)/TiO<sub>2</sub> nanocomposites in Figure 1, implying that the TiO<sub>2</sub> was enwrapped by the polymer [29].

### 2.2. Ultraviolet-Visible (UV-Vis) Absorption Spectra

The UV-Vis spectra of solid-state synthesized PProDOT/TiO<sub>2</sub>, PProDOT-Me<sub>2</sub>/TiO<sub>2</sub>, poly(TPT)/TiO<sub>2</sub> and poly(TMPT)/TiO<sub>2</sub> in N-methylpyrrolidone (NMP) are shown in Figure 2. As shown in Figure 2, PProDOT/TiO<sub>2</sub> displays a broad peak ranging from ~430 nm to 610 nm with several shoulders at ~430, ~450, ~500, ~560 and ~610 nm, while the PProDOT-Me<sub>2</sub>/TiO<sub>2</sub>, poly(TPT)/TiO<sub>2</sub> and poly(TMPT)/TiO<sub>2</sub>

display relatively sharp peaks ranging from  $\sim 460$  nm to  $\sim 610$  nm with several shoulders at  $\sim 460$ ,  $\sim 500$ ,  $\sim 554$  and  $\sim 610$  nm. The absorption peaks and shoulders at  $\sim 430$ – $560$  nm are assigned to the  $\pi \rightarrow \pi^*$  transition of the thiophene ring [30–33], while the peaks at  $\sim 610$  nm are the p-doping peaks of the polythiophene molecular chains [34]. Comparing with the absorption spectra of others, more shoulders appear in the PProDOT/TiO<sub>2</sub> nanocomposite, which can be considered as the absorption peaks arising from conjugated segments having different conjugation lengths [35]. Furthermore, the peak of the PProDOT-Me<sub>2</sub>/TiO<sub>2</sub> nanocomposite at  $\sim 500$  nm is red shifted to  $\sim 523$  nm in the poly(TMPT)/TiO<sub>2</sub> nanocomposite. Generally, the red shift of the absorption spectrum shows the increase of the conjugated chain length [36]. Moreover, the peak of poly(TPT)/TiO<sub>2</sub> appears at a relatively lower wavelength compared to the poly(TMPT)/TiO<sub>2</sub>, which is mostly originated from the strong interaction between the TiO<sub>2</sub> particles and the poly(TMPT) [37].

**Figure 1.** The Fourier transform infrared (FTIR), spectra of (a) poly(3,4-propylenedioxythiophene) (PProDOT)/TiO<sub>2</sub>; (b) PProDOT-Me<sub>2</sub>/TiO<sub>2</sub>; (c) poly(3,4-propylenedioxy-2,2':5',2''-terthiophene (TPT))/TiO<sub>2</sub> and (d) poly(3,4-(2,2-dimethylenepropylenedioxy)-2,2':5',2''-terthiophene(TMPT))/TiO<sub>2</sub>. The inset shows the spectrum of nano-TiO<sub>2</sub>.

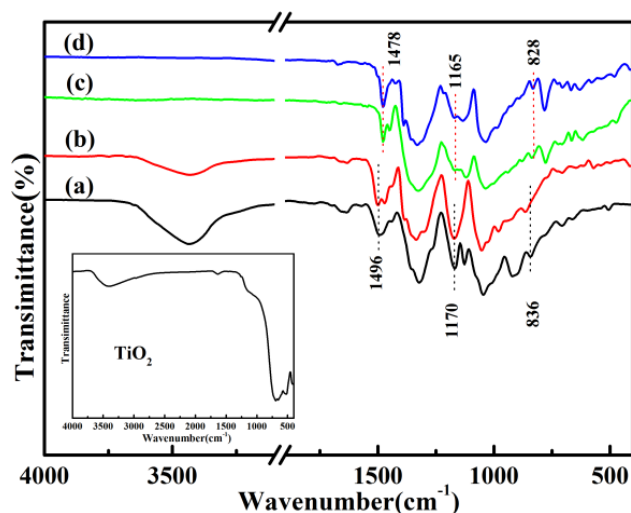
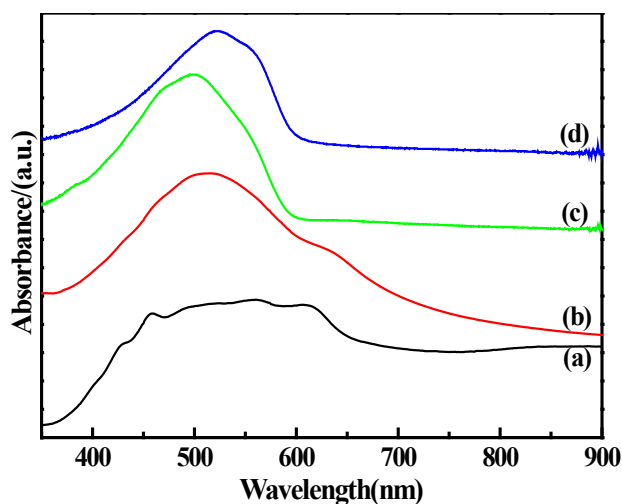


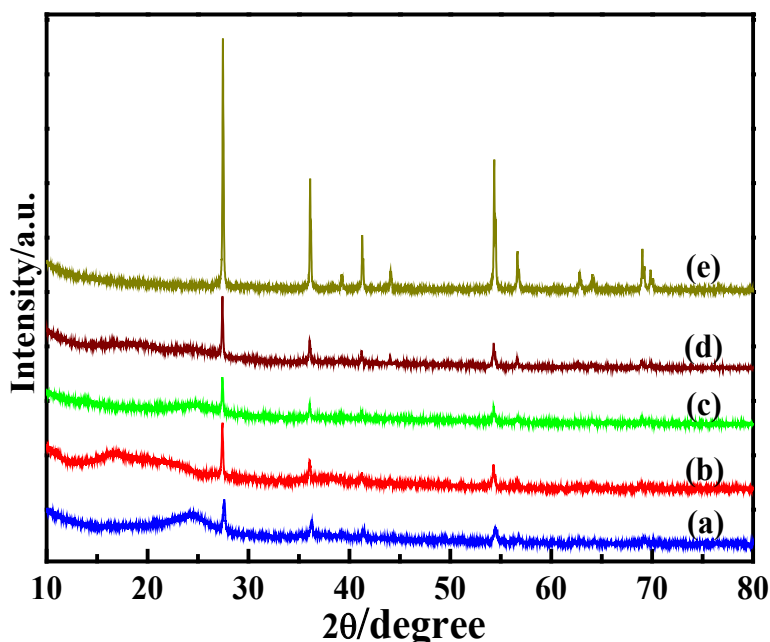
**Figure 2.** Ultraviolet-visible (UV-Vis) spectra of (a) PProDOT/TiO<sub>2</sub>; (b) PProDOT-Me<sub>2</sub>/TiO<sub>2</sub>; (c) poly(TPT)/TiO<sub>2</sub> and (d) poly(TMPT)/TiO<sub>2</sub>; in *N*-methylpyrrolidone (NMP).



### 2.3. X-ray Diffraction Patterns and Energy Dispersive X-ray Spectroscopy (EDX) Analysis

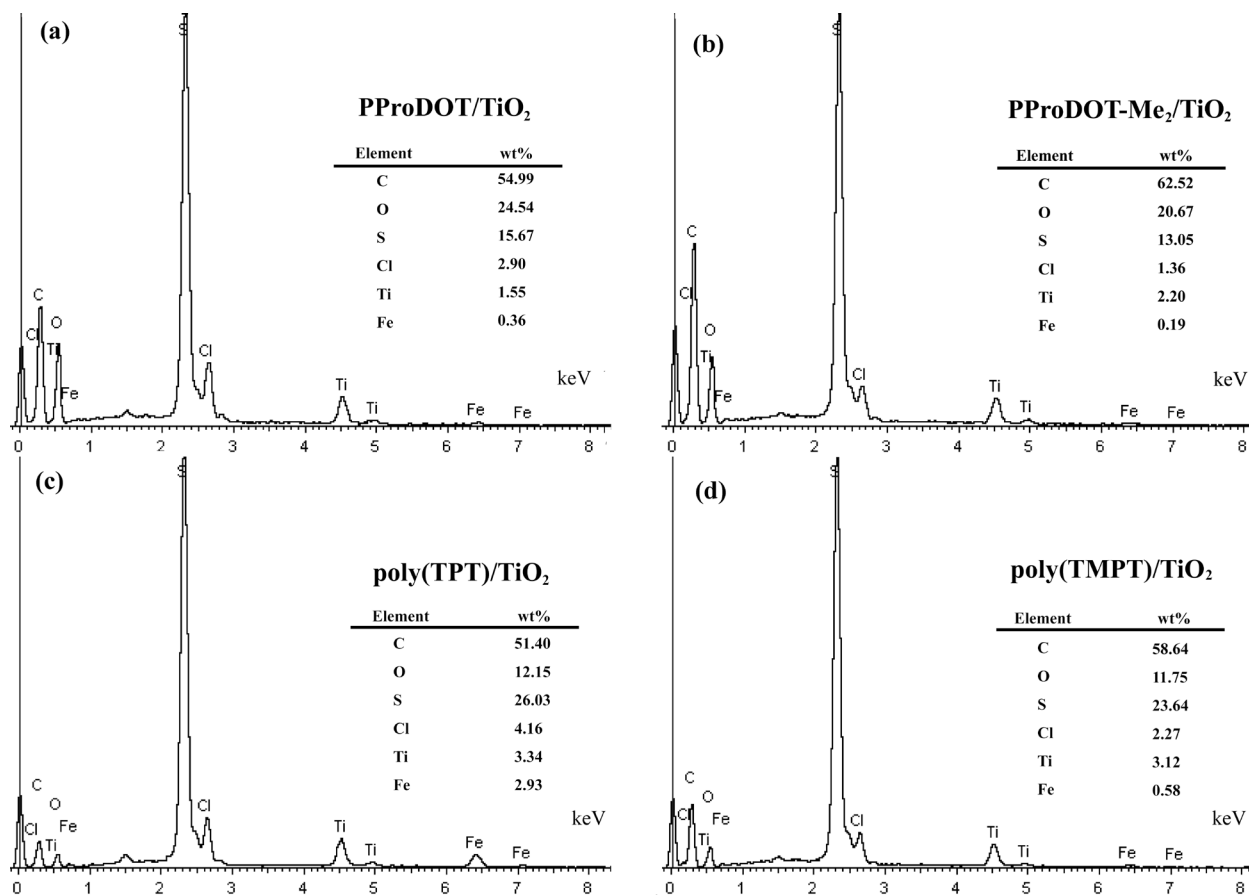
Figure 3 shows the XRD patterns of solid-state synthesized PProDOT/TiO<sub>2</sub>, PProDOT-Me<sub>2</sub>/TiO<sub>2</sub>, poly(TPT)/TiO<sub>2</sub>, poly(TMPT)/TiO<sub>2</sub> and nano-TiO<sub>2</sub>, respectively. As seen from Figure 3, the composites possess rather broad diffraction peaks, suggesting a small degree of crystallinity, but an amorphous structure, which is similar to other thiophene derivatives [38], and its diffraction peaks are located at about  $2\theta \sim 24.4^\circ$  (associated with the intermolecular  $\pi \rightarrow \pi^*$  stacking or assigned to the (020) reflection) [39] and  $2\theta \sim 37.5^\circ$  (assigned to the (111) reflection [40,41]). The XRD patterns of composites shows the presence of the characteristic diffraction peaks of rutile TiO<sub>2</sub> ( $\sim 27.6^\circ$ ,  $36.1^\circ$ ,  $41.3^\circ$ ,  $54.4^\circ$ ,  $56.7^\circ$  and  $69.5^\circ$ ), suggesting the successful incorporation of rutile TiO<sub>2</sub>. Figure 3 implies that the poly(TMPT)/TiO<sub>2</sub> nanocomposite has lower crystallinity than others. This can be associated with the introduction of dimethyl substituents in the PProDOT or poly(TPT/TiO<sub>2</sub>), which may decrease the crystallinity with its separation effect on the polymer main chains [42]. However, the intensity of the characteristic diffraction peaks of TiO<sub>2</sub> is lower in the case of the PProDOT/TiO<sub>2</sub> and poly(TPT)/TiO<sub>2</sub> nanocomposites than that of PProDOT-Me<sub>2</sub>/TiO<sub>2</sub> and poly(TMPT)/TiO<sub>2</sub>, suggesting that the TiO<sub>2</sub> particles are uniformly embedded in the polymer matrix of PProDOT/TiO<sub>2</sub> and poly(TPT)/TiO<sub>2</sub> [43].

**Figure 3.** X-ray diffraction (XRD) patterns of (a) PProDOT/TiO<sub>2</sub>; (b) PProDOT-Me<sub>2</sub>/TiO<sub>2</sub>; (c) poly(TPT)/TiO<sub>2</sub>; (d) poly(TMPT)/TiO<sub>2</sub>; and (e) nano-TiO<sub>2</sub>.



The energy dispersive X-ray spectroscopy (EDX) analysis on each composite is presented in Figure 4. As shown in Figure 4, the elements of C, O, S, Cl, Ti and Fe are observed. Additionally, the quantitative analysis of the result of EDX indicates that the wt% of Ti in each nanocomposite is 1.55%, 2.20%, 3.34% and 3.12%, respectively, which implies that poly(TPT)/TiO<sub>2</sub> and poly(TMPT)/TiO<sub>2</sub> have a higher wt% of TiO<sub>2</sub> than that of PProDOT/TiO<sub>2</sub> and PProDOT-Me<sub>2</sub>/TiO<sub>2</sub>.

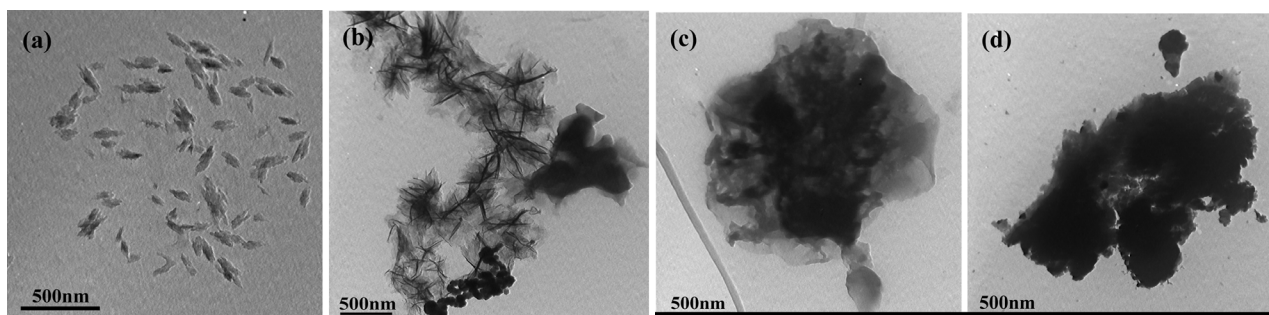
**Figure 4.** Energy dispersive X-ray spectroscopy (EDX) spectra of each composite: (a) PProDOT/TiO<sub>2</sub>; (b) PProDOT-Me<sub>2</sub>/TiO<sub>2</sub>; (c) poly(TPT)/TiO<sub>2</sub>; and (d) poly(TMPT)/TiO<sub>2</sub>.



## 2.4. Morphology

Figure 5 represents the transmission electron microscopy (TEM) images of solid-state synthesized PProDOT/TiO<sub>2</sub>, PProDOT-Me<sub>2</sub>/TiO<sub>2</sub>, poly(TPT)/TiO<sub>2</sub> and poly(TMPT)/TiO<sub>2</sub>. As shown in Figure 5, all the nanocomposites display a sponge-like morphology, except from the PProDOT/TiO<sub>2</sub> nanocomposite. Additionally, the TiO<sub>2</sub> particles (dark-shaded nanoparticles) are found to be entrapped in polymer (light shaded) matrix. These results reveal that the TiO<sub>2</sub> particles are not simply mixed up or blended with the polymer, suggesting that the TiO<sub>2</sub> particles are embedded in the polymer matrix, which is quite in accordance with the results of the XRD analysis.

**Figure 5.** Transmission electron microscopy (TEM) images of (a) PProDOT/TiO<sub>2</sub>; (b) PProDOT-Me<sub>2</sub>/TiO<sub>2</sub>; (c) poly(TPT)/TiO<sub>2</sub>; and (d) poly(TMPT)/TiO<sub>2</sub>.



### 2.5. Photocatalytic Properties

Figure 6 shows the photocatalytic degradation of methylene blue (MB) dye with the presence of the PProDOT/TiO<sub>2</sub>, PProDOT-Me<sub>2</sub>/TiO<sub>2</sub>, poly(TPT)/TiO<sub>2</sub> and poly(TMPT)/TiO<sub>2</sub> nanocomposites and pure nano-TiO<sub>2</sub> as catalysts under UV light at different irradiations time, while Figure 7 indicates the photocatalytic degradation of MB dye in the presence of the above composites and the pure nano-TiO<sub>2</sub> as the catalyst under natural sunlight at different irradiations time. Generally, the adsorption/desorption equilibrium is an important preliminary step in the photocatalytic degradation process. Therefore, prior to irradiation, the MB solution was magnetically stirred in the dark for 30 min to ensure the establishment of the adsorption/desorption equilibrium. As can be seen in Figures 6 and 7, the diminished characteristic band of MB dye at ~660 nm after 7 h under UV light and natural sunlight indicates that the MB has been degraded by all the nanocomposites and pure nano-TiO<sub>2</sub>. Additionally, the degradation efficiency of each nanocomposite is 32.5%, 29.6%, 51.5% and 44.4% under UV light for PProDOT/TiO<sub>2</sub>, PProDOT-Me<sub>2</sub>/TiO<sub>2</sub>, poly(TPT)/TiO<sub>2</sub> and poly(TMPT)/TiO<sub>2</sub>, respectively, while the degradation efficiency of each nanocomposite is 79.6%, 62.8%, 90.5% and 84.6% under natural sunlight for PProDOT /TiO<sub>2</sub>, PProDOT-Me<sub>2</sub>/TiO<sub>2</sub>, poly(TPT)/TiO<sub>2</sub> and poly(TMPT)/TiO<sub>2</sub>, respectively. In addition, the degradation efficiency of nano-TiO<sub>2</sub> under UV light and natural sunlight is 27% and 11.6%, respectively. It is easy to see that the degradation efficiency of the MB in the presence of poly(TPT)/TiO<sub>2</sub> and poly(TMPT)/TiO<sub>2</sub> is higher than that of PProDOT/TiO<sub>2</sub> and PProDOT-Me<sub>2</sub>/TiO<sub>2</sub>. Meanwhile, the degradation efficiency increased up to two and three times compared to PProDOT/TiO<sub>2</sub> and PProDOT-Me<sub>2</sub>/TiO<sub>2</sub>, respectively, under the same conditions, which suggests that the poly(TPT)/TiO<sub>2</sub> and poly(TMPT)/TiO<sub>2</sub> nanocomposites are more effective photocatalysts for the degradation of MB than the PProDOT/TiO<sub>2</sub> and PProDOT-Me<sub>2</sub>/TiO<sub>2</sub> nanocomposites.

Based on previous reports, the photocatalytic degradation of MB under UV or visible light irradiation is mainly related to the generation of reactive hydroxy and hydroperoxy radicals [44–46]. Herrmann *et al.* investigated the TiO<sub>2</sub>/UV photocatalytic degradation of MB in aqueous heterogeneous suspensions, and a detailed degradation pathway was determined by a careful identification of intermediate products, in particular aromatics, whose successive hydroxylations led to the aromatic ring opening. Furthermore, they found that TiO<sub>2</sub>/UV-based photocatalysis was simultaneously able to oxidize the MB with an almost complete mineralization of carbon and of nitrogen and sulfur heteroatoms into CO<sub>2</sub>, NH<sub>4</sub><sup>+</sup>, NO<sub>3</sub><sup>-</sup> and SO<sub>4</sub><sup>2-</sup>, respectively [47]. According to the reports, the hydroxy and hydroperoxy radicals produced by the action of photocatalyst are capable of oxidizing MB molecules at the surface layer of photocatalyst. MB molecules tend to be adsorbed by the surface of the catalyst. This process can be enhanced by controlling the surface charge of the photocatalyst. Moreover, MB is a cationic dye, and a negatively charged photocatalyst surface accelerates the adsorption of the MB and, consequently, the photo degradation process [44,45].

As can be seen in Figure 7, almost complete degradation of the MB has been achieved 7 h under natural light irradiation using nanocomposites as the photocatalyst, except from the PProDOT-Me<sub>2</sub>/TiO<sub>2</sub> nanocomposites. In addition, the degradation efficiency of both poly(TPT)/TiO<sub>2</sub> and poly(TMPT)/TiO<sub>2</sub> are higher than that of PProDOT/TiO<sub>2</sub> and PProDOT-Me<sub>2</sub>/TiO<sub>2</sub>. To summarize, the poly(TPT)/TiO<sub>2</sub> and poly(TMPT)/TiO<sub>2</sub> nanocomposites had higher degradation efficiencies than the PProDOT/TiO<sub>2</sub> and PProDOT-Me<sub>2</sub>/TiO<sub>2</sub> nanocomposites under both light sources. Moreover, the degradation

efficiency of all nanocomposites under sunlight are much higher than under UV light, which indicates that the nanocomposites are more effective photocatalysts for the degradation of MB under the higher intensity of sunlight irradiation than UV irradiation.

**Figure 6.** The UV-Vis absorption spectra of methylene blue (MB) dyes by photocatalysis for different irradiation times under UV light irradiation: (a) PProDOT/TiO<sub>2</sub>; (b) PProDOT-Me<sub>2</sub>/TiO<sub>2</sub>; (c) poly(TPT)/TiO<sub>2</sub>; (d) poly(TMPT)/TiO<sub>2</sub>; (e) Nano-TiO<sub>2</sub>; and (f) the degradation efficiency of the MB dyes (catalyst concentration: 0.4 mg/mL; initial concentration of dyes:  $1 \times 10^{-5}$  M).

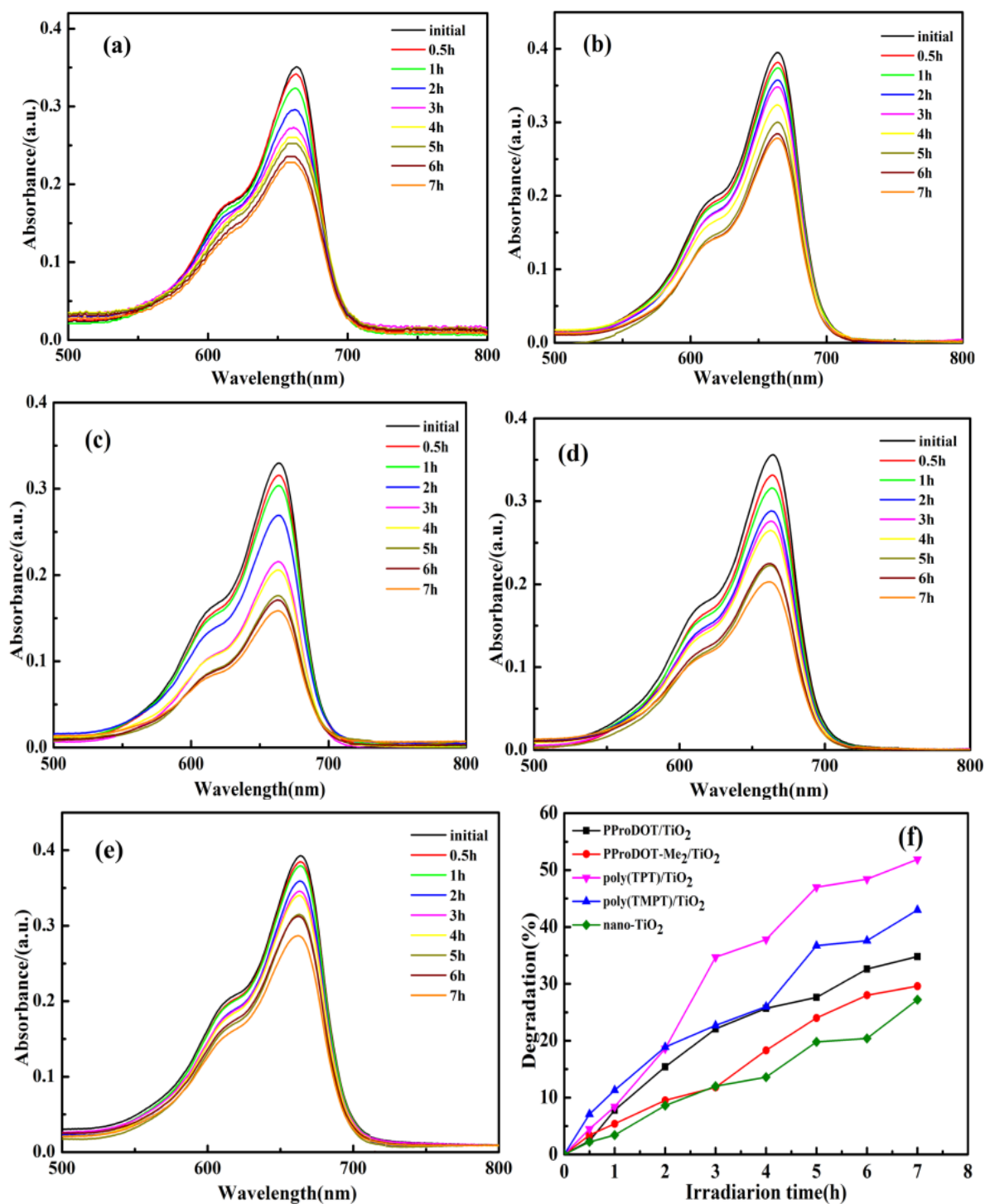


**Figure 7.** The UV-Vis absorption spectra of MB dyes by photocatalysis for different irradiation times under sunlight irradiation: (a) PProDOT/TiO<sub>2</sub>; (b) PProDOT-Me<sub>2</sub>/TiO<sub>2</sub>; (c) poly(TPT)/TiO<sub>2</sub>; (d) poly(TMPT)/TiO<sub>2</sub>; (e) Nano-TiO<sub>2</sub>; and (f) the degradation efficiency of the MB dyes (catalyst concentration: 0.4 mg/mL; initial concentration of dyes:  $1 \times 10^{-5}$  M).

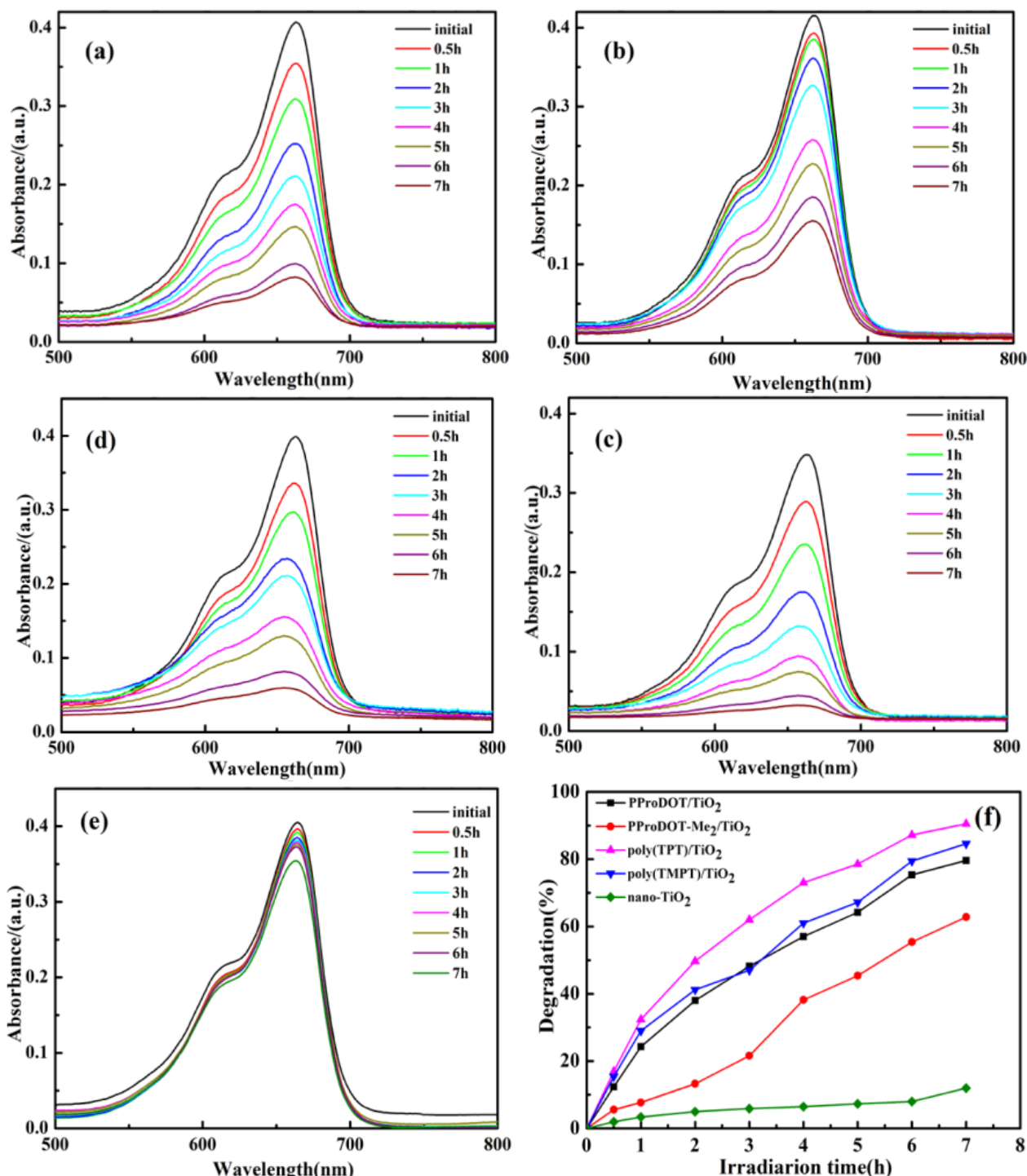
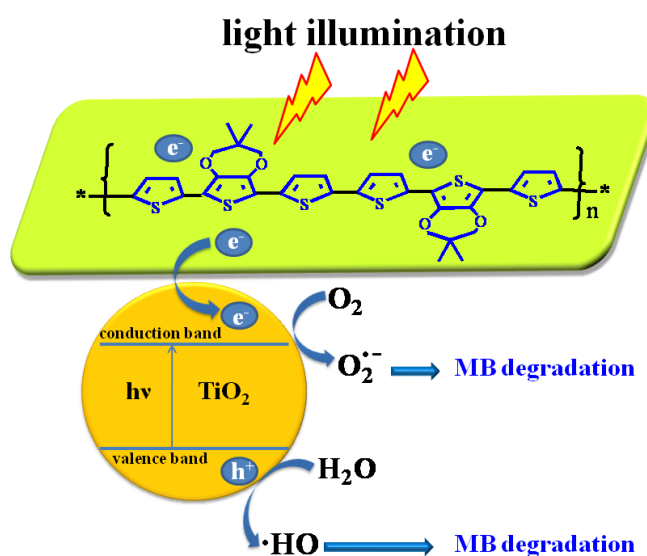


Figure 8 shows the schematic mechanism of MB dye degradation to explain the photocatalytic activity of the nanocomposite catalyst under sunlight. According to the previous report, TiO<sub>2</sub> particles can absorb UV light to create electrons (e<sup>-</sup>) in the conduction band and holes (h<sup>+</sup>) in the valence band [48], respectively. If the electrons and holes cannot be captured in time, they will recombine with

each other within a few nanoseconds, which will reduce the photocatalytic efficiency of  $\text{TiO}_2$ . However, in the case of composites, due to the existence of the interface between polymer and  $\text{TiO}_2$ , separated electrons and holes have little possibility to recombine again. This ensures higher charge separation efficiency and better photo-oxidation capacity for the nanocomposite. In addition, the polymer can absorb the visible light and produces an electron ( $e^-$ ) that transfers to the conduction band of  $\text{TiO}_2$  [48,49]. The amount of  $\cdot\text{OH}$  and  $\text{O}_2^{\cdot-}$  formed in the case of composites is more than that with  $\text{TiO}_2$  alone as a photocatalyst. Moreover, MB molecules can transfer from solution to the catalyst's surface and be adsorbed with an offset face-to-face orientation via  $\pi$ - $\pi$  conjugation between MB and aromatic regions of the polymer, and therefore, the adsorptivity of MB on polymer increases compared to that of MB on bare  $\text{TiO}_2$ , which makes the composites have a higher efficiency in the photodegradation of MB compared to  $\text{TiO}_2$  alone as a photocatalyst.

**Figure 8.** A schematic illustration of the photocatalytic activity of a nanocomposite (take the poly(TMPT)/ $\text{TiO}_2$  nanocomposite for example).



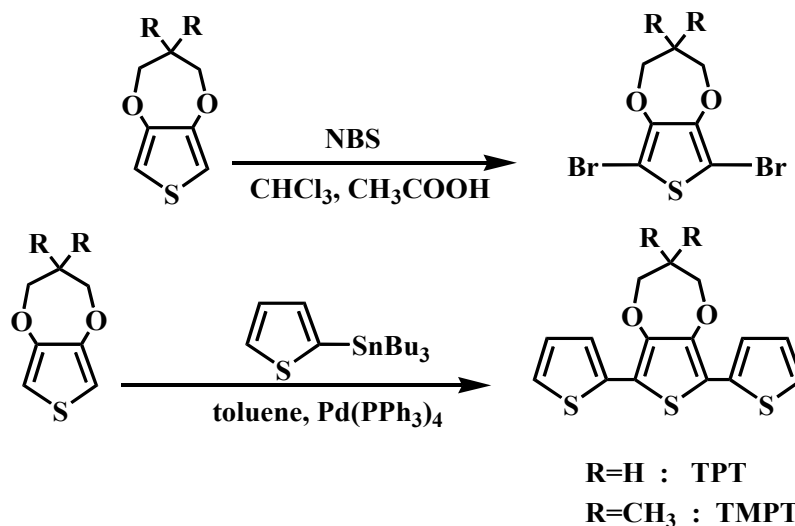
### 3. Experimental Section

#### 3.1. Materials

2-(tributylstannyl)-thiophene, *N*-bromo-succinimide (NBS), 3,4-propylenedioxythiophene (ProDOT), 3,4-(2,2-dimethylenepropylenedioxy)thiophene(ProDOT- $\text{Me}_2$ ) and anhydrous iron(III) chloride were obtained from Aldrich (Tokyo, Japan) and used as received.  $\text{Pd}(\text{PPh}_3)_4$  was synthesized according to the literature [50,51]. The nano- $\text{TiO}_2$  (rutile, lipophilic, with an average size of 100 nm, Shanghai Aladdin Reagent Company, Shanghai, China) and all other chemicals were used as received without further purification.

#### 3.2. Preparation of Monomers

3,4-propylenedioxy-2,2':5',2''-terthiophene(TPT) and 3,4-(2,2-dimethylenepropylene-dioxy)-2,2':5',2''-terthiophene(TMPT) were synthesized according to the procedure given in [42], as shown in Scheme 1.

**Scheme 1.** Synthesis of monomers (TPT and TMPT).

### 3.3. Preparation of Composites

A typical solid-state synthesis procedure of the composite was as follows: a mixture of 0.3 g (0.9 mmol) 3,4-propylenedioxy-2,2':5',2''-terthiophene (TPT) and 15 mg  $\text{TiO}_2$  in 3 mL chloroform were ultrasonicated for 30 min to facilitate the monomer in adsorbing onto the surface of  $\text{TiO}_2$ . After ultrasonication, the mixture was allowed to evaporate the chloroform, then the mixture was put in a mortar, and 0.61 g (3.6 mmol) anhydrous iron(III) chloride ( $\text{FeCl}_3$ ) were added to this mixture, then ground for 1 h. Then, the mixture was washed with chloroform, ethanol and distilled water, respectively, until the filtrate was colorless, finally drying the powder under vacuum at 60 °C for 48 h. The obtained composite was denoted as poly(TPT)/ $\text{TiO}_2$ . Poly(TMPT)/ $\text{TiO}_2$  was synthesized in a similar manner by keeping the ratio of  $[\text{TMPT}]/[\text{FeCl}_3]$  at 1:4.

The other composites, poly(3,4-propylenedioxythiophene)/ $\text{TiO}_2$  nanocomposite (PProDOT/ $\text{TiO}_2$ ) and poly(3,4-(2,2-dimethylenepropylenedioxy)thiophene)/ $\text{TiO}_2$  composite (PProDOT/ $\text{TiO}_2$ ), were obtained in a similar manner by keeping the ratio of  $[\text{monomer}]/[\text{FeCl}_3]$  at 1:4.

### 3.4. Structure Characterization

The Fourier transform infrared (FTIR) spectra of the composite were obtained by using a BRUKERQEUNOX-55 Fourier transform infrared spectrometer (Billerica, MA, USA) (frequency range: 4000–500  $\text{cm}^{-1}$ ). The UV-Vis spectra and photocatalytic activity of the samples were recorded on a UV-Visible spectrophotometer (UV4802, Unico, Franksville, WI, USA). X-ray powder diffraction (XRD) patterns were obtained by using a Bruker AXS D8 diffractometer (Bruker AXS Co., Karlsruhe, Germany), with a monochromatic Cu-K $\alpha$  radiation source ( $\lambda = 0.15418$ ). The scan range ( $2\theta$ ) was 5°–80°. Transmission electron microscopy (TEM) experiments were carried out in a Hitachi 2600 electron microscope (Tokyo, Japan). The samples for TEM measurements were prepared by placing a few drops of sample ethanol suspension on copper supports.

### 3.5. Measurement of Photocatalytic Activities

The photocatalytic activities of nanocomposites were performed using MB as degraded materials in quartz tubes under UV light and natural sunlight irradiation. FSL MW1-Y15 (Royal Dutch Philips Electronics Ltd., Amsterdam, The Netherlands) was used as the irradiation source ( $\lambda = 254$  nm) located in a light infiltrated chamber. Before irradiation, the suspension was stirred magnetically for 30 min in dark conditions until an adsorption-desorption equilibrium was established. Then, the suspensions were irradiated by light sources. Under natural sunlight investigations, all experiments were done inside a laboratory in an open atmosphere in the month of September. The photodegradation efficiency ( $R$ , %) was calculated by use of the following equation:  $R = [C_0 - C/C_0]$  (where  $C_0$  represents the concentration of the dye before illumination and  $C$  denotes the concentration of dye after a certain irradiation time, respectively).

## 4. Conclusions

In this paper, the polyterthiophene derivatives/TiO<sub>2</sub> nanocomposites, such as poly(3,4-propylenedioxy-2,2':5',2''-terthiophene)/TiO<sub>2</sub> nanocomposite (poly(TPT)/TiO<sub>2</sub>) and poly(3,4-(2,2-dimethylenepropylenedioxy)-2,2':5',2''-terthiophene)/TiO<sub>2</sub> nanocomposite (poly(TMPT)/TiO<sub>2</sub>), were synthesized by a simple solid-state method. The poly(3,4-propylenedioxythiophene)/TiO<sub>2</sub> nanocomposite (PProDOT/TiO<sub>2</sub>) and poly(3,4-2,2-dimethylenepropylenedioxythiophene)/TiO<sub>2</sub> nanocomposite (PProDOT-Me<sub>2</sub>/TiO<sub>2</sub>) were synthesized by the same method for comparison. The results showed that the higher oxidation degree and the strong interaction between TiO<sub>2</sub> and polymer occurred in the case of poly(TPT)/TiO<sub>2</sub> and poly(TMPT)/TiO<sub>2</sub> compared with that of PProDOT/TiO<sub>2</sub> and PProDOT-Me<sub>2</sub>/TiO<sub>2</sub>. This phenomenon mainly resulted from the linear growth tendency of terthiophene-type monomers, which made the whole polyterthiophene-type chain grow regularly and led to an enhancement of the electronic and optical properties of the nanocomposites. The results also indicated that TiO<sub>2</sub> had no effect on the crystallinity of the polymer, but TiO<sub>2</sub> can be embedded in the polymer matrix, which implied that the solid-state method can be an effective method for preparing such composite materials. Furthermore, the UV-Vis photodegradation efficiency of MB by these composites showed that the poly(TPT)/TiO<sub>2</sub> and poly(TMPT)/TiO<sub>2</sub> nanocomposites had higher degradation efficiency than that of the PProDOT/TiO<sub>2</sub> and PProDOT-Me<sub>2</sub>/TiO<sub>2</sub> nanocomposites, which resulted from the positive effect of the higher oxidation degree of the polyterthiophene derivatives/TiO<sub>2</sub> nanocomposites, as well as the strong interaction between TiO<sub>2</sub> and the polyterthiophene derivatives than that of PProDOT/TiO<sub>2</sub> and PProDOT-Me<sub>2</sub>/TiO<sub>2</sub>. The photodegradation studies suggested that the polyterthiophene derivatives/TiO<sub>2</sub> nanocomposites were more effective photocatalysts for the degradation of MB under UV and sunlight irradiation. All nanocomposites were more effective photocatalysts as compared to bare TiO<sub>2</sub>, because the polymers acted as light-harvesting species, and the polymers displayed a positive role in charge separation, except the adsorption effect of polymers for MB via  $\pi$ - $\pi$  conjugation between MB and aromatic regions of the polymer.

## Acknowledgments

We gratefully acknowledge the financial support from the National Natural Science Foundation of China (No. 21064007, No. 21264014) and the Opening Project of Xinjiang Laboratory of Petroleum and Gas Fine Chemicals (XJDX0908-2011-05).

## Author Contributions

Ruxangul Jamal designed the experiments, and edited the paper. Yakupjan Osman carried out the experiments, Adalet Rahman, Ahmet Ali, and Yu Zhang advised about the scientific meanings of this study and edited the paper. Tursun Abdiryim directed, carried out the experiments and wrote the paper.

## Conflicts of Interest

The authors declare no conflict of interest.

## References

1. Morán-pineda, M.; Castillo, S.; Asomoza, M.; Gómez, R. Al<sub>2</sub>O<sub>3</sub>-TiO<sub>2</sub> sol-gel mixed oxides as suitable supports for the reduction of NO by CO. *React. Kinet. Catal. Lett.* **2002**, *76*, 75–81.
2. Park, E.J.; Jeong, B.; Jeong, M.-G.; Kim, Y.D. Synergetic effects of hydrophilic surface modification and N-doping for visible light response on photocatalytic activity of TiO<sub>2</sub>. *Curr. Appl. Phys.* **2014**, *14*, 300–305.
3. Patel, N.; Jaiswal, R.; Warang, T.; Scarduelli, G.; Dashora, A.; Ahuja, B.L.; Kothari, D.C.; Miotello, A. Efficient photocatalytic degradation of organic water pollutants using V–N-codoped TiO<sub>2</sub> thin films. *Appl. Catal. B Environ.* **2014**, *150–151*, 74–81.
4. Mohamed, R. Characterization and catalytic properties of nano-sized Pt metal catalyst on TiO<sub>2</sub>-SiO<sub>2</sub> synthesized by photo-assisted deposition and impregnation methods. *J. Mater. Process. Technol.* **2009**, *209*, 577–583.
5. Gu, D.-E.; Yang, B.-C.; Hu, Y.-D. A novel method for preparing V-doped titanium dioxide thin film photocatalysts with high photocatalytic activity under visible light irradiation. *Catal. Lett.* **2007**, *118*, 254–259.
6. Yan, X.; He, J.; Evans, D.G.; Duan, X.; Zhu, Y. Preparation, characterization and photocatalytic activity of Si-doped and rare earth-doped TiO<sub>2</sub> from mesoporous precursors. *Appl. Catal. B Environ.* **2005**, *55*, 243–252.
7. Lock, J.P.; Lutkenhaus, J.L.; Zacharia, N.S.; Im, S.G.; Hammond, P.T.; Gleason, K.K. Electrochemical investigation of PEDOT films deposited via CVD for electrochromic applications. *Synth. Met.* **2007**, *157*, 894–898.
8. Zhang, L.; Liu, P.; Su, Z. Preparation of PANI–TiO<sub>2</sub> nanocomposites and their solid-phase photocatalytic degradation. *Polym. Degrad. Stab.* **2006**, *91*, 2213–2219.
9. Uygun, A.; Turkoglu, O.; Sen, S.; Ersoy, E.; Yavuz, A.G.; Batir, G.G. The electrical conductivity properties of polythiophene/TiO<sub>2</sub> nanocomposites prepared in the presence of surfactants. *Curr. Appl. Phys.* **2009**, *9*, 866–871.

10. Xu, S.H.; Li, S.Y.; Wei, Y.X.; Zhang, L.; Xu, F. Improving the photocatalytic performance of conducting polymer polythiophene sensitized TiO<sub>2</sub> nanoparticles under sunlight irradiation. *React. Kinet. Mech. Catal.* **2010**, *101*, 237–249.
11. Xu, S.; Jiang, L.; Yang, H.; Song, Y.; Dan, Y. Structure and photocatalytic activity of polythiophene/TiO<sub>2</sub> composite particles prepared by photoinduced polymerization. *Chin. J. Catal.* **2011**, *32*, 536–545.
12. Dehaut, J.; Beouch, L.; Peralta, S.; Plesse, C.; Aubert, P.H.; Chevrot, C.; Goubard, F. Facile route to prepare film of poly(3,4-ethylene dioxythiophene)-TiO<sub>2</sub> nanohybrid for solar cell application. *Thin Solid Films* **2011**, *519*, 1876–1881.
13. Ma, L.; Li, Y.; Yu, X.; Yang, Q.; Noh, C.-H. Using room temperature ionic liquid to fabricate PEDOT/TiO<sub>2</sub> nanocomposite electrode-based electrochromic devices with enhanced long-term stability. *Sol. Energy Mater. Sol. Cells* **2008**, *92*, 1253–1259.
14. Muktha, B.; Mahanta, D.; Patil, S.; Madras, G. Synthesis and photocatalytic activity of poly(3-hexylthiophene)/TiO<sub>2</sub> composites. *J. Solid State Chem.* **2007**, *180*, 2986–2989.
15. Yamamoto, T.; Sanechika, K.-I.; Yamamoto, A. Preparation and characterization of poly(thienylene)s. *Bull. Chem. Soc. Jpn.* **1983**, *56*, 1497–1502.
16. Roncali, J. Synthetic principles for bandgap control in linear  $\pi$ -conjugated systems. *Chem. Rev.* **1997**, *97*, 173–206.
17. Meerholz, K.; Heinze, J. Electrochemical solution and solid-state investigations on conjugated oligomers and polymers of the  $\alpha$ -thiophene and the p-phenylene series. *Electrochim. Acta* **1996**, *41*, 1839–1854.
18. Tsekouras, G.; Too, C.O.; Wallace, G.G. Effect of growth conditions on the photovoltaic efficiency of poly(terthiophene) based photoelectrochemical cells. *Electrochim. Acta* **2005**, *50*, 3224–3230.
19. Zanardi, C.; Scanu, R.; Pigani, L.; Pilo, M.I.; Sanna, G.; Seeber, R.; Spano, N.; Terzi, F.; Zucca, A. Synthesis and electrochemical polymerisation of 3'-functionalised terthiophenes: Electrochemical and spectroelectrochemical characterisation. *Electrochim. Acta* **2006**, *51*, 4859–4864.
20. Abdiryim, T.; Jamal, R.; Zhao, C.; Awut, T.; Nurulla, I. Structure and properties of solid-state synthesized poly(3'4'-ethylenedioxy-2,2':5',2"-terthiophene). *Synth. Met.* **2010**, *160*, 325–332.
21. Yang, Y.; Jiang, Y.; Xu, J.; Yu, J. Conducting polymeric nanoparticles synthesized in reverse micelles and their gas sensitivity based on quartz crystal microbalance. *Polymer* **2007**, *48*, 4459–4465.
22. Kim, Y.S.; Oh, S.B.; Park, J.H.; Cho, M.S.; Lee, Y. Highly conductive PEDOT/silicate hybrid anode for ITO-free polymer solar cells. *Sol. Energy Mater. Sol. Cells* **2010**, *94*, 471–477.
23. Cloutet, E.; Mumtaz, M.; Cramail, H. Synthesis of PEDOT latexes by dispersion polymerization in aqueous media. *Mater. Sci. Eng. C* **2009**, *29*, 377–382.
24. Reddy, K.R.; Park, W.; Sin, B.C.; Noh, J.; Lee, Y. Synthesis of electrically conductive and superparamagnetic monodispersed iron oxide-conjugated polymer composite nanoparticles by *in situ* chemical oxidative polymerization. *J. Colloid Interface Sci.* **2009**, *335*, 34–39.
25. Shin, H.J.; Jeon, S.S.; Im, S.S. CNT/PEDOT core/shell nanostructures as a counter electrode for dye-sensitized solar cells. *Synth. Met.* **2011**, *161*, 1284–1288.

26. Kumar, N.A.; Choi, H.J.; Bund, A.; Baek, J.-B.; Jeong, Y.T. Electrochemical supercapacitors based on a novel graphene/conjugated polymer composite system. *J. Mater. Chem.* **2012**, *22*, 12268–12274.
27. Sindhu, S.; Siju, C.; Sharma, S.; Rao, K.; Gopal, E. Optical, electrochemical and morphological investigations of poly(3,4-propylenedioxythiophene)–sultone (PProDOT–S) thin films. *Bull. Mater. Sci.* **2012**, *35*, 611–616.
28. Abdiryim, T.; Ubul, A.; Jamal, R.; Xu, F.; Rahman, A. Electrochemical properties of the poly(3,4-ethylenedioxythiophene)/single-walled carbon nanotubes composite synthesized by solid-state heating method. *Synth. Met.* **2012**, *162*, 1604–1608.
29. Abdiryim, T.; Ubul, A.; Jamal, R.; Tian, Y.; Awut, T.; Nurulla, I. Solid-state synthesis and characterization of polyaniline/nano-TiO<sub>2</sub> composite. *J. Appl. Polym. Sci.* **2012**, *126*, 697–705.
30. Kvarnström, C.; Neugebauer, H.; Blomquist, S.; Ahonen, H.; Kankare, J.; Ivaska, A. *In situ* spectroelectrochemical characterization of poly(3,4-ethylenedioxythiophene). *Electrochim. Acta* **1999**, *44*, 2739–2750.
31. Han, M.G.; Foulger, S.H. Facile synthesis of poly(3,4-ethylenedioxythiophene) nanofibers from an aqueous surfactant solution. *Small* **2006**, *2*, 1164–1169.
32. Fall, M.; Aaron, J.; Sakmeche, N.; Dieng, M.; Jouini, M.; Aeiyaach, S.; Lacroix, J.; Lacaze, P. Electrochemical and spectroscopic properties of poly(3-methoxythiophene) electrosynthesized in an aqueous micellar medium. *Synth. Met.* **1998**, *93*, 175–179.
33. Yamamoto, T.; Shimizu, T.; Kurokawa, E. Doping behavior of water-soluble  $\pi$ -conjugated polythiophenes depending on pH and interaction of the polymer with DNA. *React. Funct. Polym.* **2000**, *43*, 79–84.
34. Abdiryim, T.; Zhao, C.; Jamal, R.; Ubul, A.; Shi, W.; Nurulla, I. The effect of solvents and organic acids on the p-doping behaviors of poly (3',4'-Ethylenedioxy-2,2':5',2"-terthiophene). *Polym. Sci. Ser. B* **2012**, *54*, 413–419.
35. Apperloo, J.J.; Janssen, R.; Nielsen, M.M.; Bechgaard, K. Doping in solution as an order-inducing tool prior to film formation of regio-irregular polyalkylthiophenes. *Adv. Mater.* **2000**, *12*, 1594–1597.
36. An, S.; Abdiryim, T.; Ding, Y.; Nurulla, I. A comparative study of the microemulsion and interfacial polymerization for polyindole. *Mater. Lett.* **2008**, *62*, 935–938.
37. Yang, J.; Zhao, X.; Shan, X.; Fan, H.; Yang, L.; Zhang, Y.; Li, X. Blue-shift of UV emission in ZnO/graphene composites. *J. Alloys Compd.* **2013**, *556*, 1–5.
38. Vacca, P.; Nenna, G.; Miscioscia, R.; Palumbo, D.; Minarini, C.; Sala, D.D. Patterned Organic and Inorganic Composites for Electronic Applications. *J. Phys. Chem. C* **2009**, *113*, 5777–5783.
39. Kim, T.Y.; Park, C.M.; Kim, J.E.; Suh, K.S. Electronic, chemical and structural change induced by organic solvents in tosylate-doped poly(3,4-ethylenedioxythiophene)(PEDOT-OTs). *Synth. Met.* **2005**, *149*, 169–174.
40. Arbizzani, C.; Bisio, M.; Manferrari, E.; Mastragostino, M. Methanol oxidation by pEDOT-pSS/PtRu in DMFC. *J. Power Sources* **2008**, *178*, 584–590.
41. Cho, M.S.; Kim, S.Y.; Nam, J.D.; Lee, Y. Preparation of PEDOT/Cu composite film by *in situ* redox reaction between EDOT and copper(II) chloride. *Synth. Met.* **2008**, *158*, 865–869.

42. Abdiryim, T.; Jamal, R.; Ubul, A.; Nurulla, I. Solid-state synthesis of poly(3',4'-dimethoxy-2,2':5',2"-terthiophene): Comparison with poly(terthiophene) and poly(3',4'-ethylenedioxy-2,2':5',2"-terthiophene). *Molecules* **2012**, *17*, 8647–8660.
43. Wang, F.; Min, S.X. TiO<sub>2</sub>/polyaniline composites: An efficient photocatalyst for the degradation of methylene blue under natural light. *Chin. Chem. Lett.* **2007**, *18*, 1273–1277.
44. Tschirch, J.; Dillert, R.; Bahnemann, D.; Proft, B.; Biedermann, A.; Goer, B. Photodegradation of methylene blue in water, a standard method to determine the activity of photocatalytic coatings? *Res. Chem. Intermed.* **2008**, *34*, 381–392.
45. Fu, P.-F.; Zhao, Z.; Peng, P.; Dai, X.-G. Photodegradation of methylene blue in a batch fixed bed photoreactor using activated carbon fibers supported TiO<sub>2</sub> photocatalyst. *Chin. J. Process Eng.* **2008**, *8*, 65–71.
46. Kim, J.; Choi, W.; Park, H. Effects of TiO<sub>2</sub> surface fluorination on photocatalytic degradation of methylene blue and humic acid. *Res. Chem. Intermed.* **2010**, *36*, 127–140.
47. Houas, A.; Lachheb, H.; Ksibi, M.; Elaloui, E.; Guillard, C.; Herrmann, J.-M. Photocatalytic degradation pathway of methylene blue in water. *Appl. Catal. B Environ.* **2001**, *31*, 145–157.
48. Wang, S.; Qian, H.; Hu, Y.; Dai, W.; Zhong, Y.; Chen, J.; Hu, X. Facile one-pot synthesis of uniform TiO<sub>2</sub>-Ag hybrid hollow spheres with enhanced photocatalytic activity. *Dalton Trans.* **2013**, *42*, 1122–1128.
49. Zhu, S.; Wei, W.; Chen, X.; Jiang, M.; Zhou, Z. Hybrid structure of polyaniline/ZnO nanograss and its application in dye-sensitized solar cell with performance improvement. *J. Solid State Chem.* **2012**, *190*, 174–179.
50. Meng, H.; Perepichka, D.F.; Bendikov, M.; Wudl, F.; Pan, G.Z.; Yu, W.; Dong, W.; Brown, S. Solid-state synthesis of a conducting polythiophene via an unprecedented heterocyclic coupling reaction. *J. Am. Chem. Soc.* **2003**, *125*, 15151–15162.
51. Kanbara, T.; Miyazaki, Y.; Yamamoto, T. New  $\pi$ -conjugated heteroaromatic alternative copolymers with electron-donating thiophene or furan units and electron-withdrawing quinoxaline units: Preparation by palladium-catalyzed polycondensation and characterization of the copolymers. *J. Polym. Sci. Part A Polym. Chem.* **1995**, *33*, 999–1003.